

BER estimation for STBC-MC-DS-CDMA-4 antennas system by varied wavelet-carriers features via AWGN-flat channels

Nader Abdullah Khadim¹, Ali Jawad Kadhim Jawad Alrubaie², Osama Qasim Jumah Al-Thahab³

¹Medical Instrumentation Techniques Engineering, Al-Mustaqbal University College, Hillah, Iraq

²College of engineering, University of Babylon, Hillah, Iraq

³Department of Electrical, College of Engineering, University of Babylon, Hillah, Iraq

Article Info

Article history:

Received Nov 29, 2022

Revised Apr 17, 2023

Accepted May 10, 2023

Keywords:

Bit error rate enhancement

Code division multiple access

Fast fourier transform

Orthogonal frequency-division

multiplexing

Wavelet transform

ABSTRACT

This paper improves the bit error rate (BER) of the modern communication system by taking into account the effect of the wavelet shape and the number of carriers on the performance of the space time block code multi-carrier direct sequence code division multiple access (STBC-MC-DS-CDMA). Here the transmitter is moved with speeds 2 km/hr, 45 km/hr and 100 km/hr via Rayleigh flat fading channel. Here, 2 antennas are employed at the receiver to mitigate the multipath signal influence. The system's orthogonal frequencies are generated using Haar, Daubechies 4, Symlets 4, Cohen-Daubechies-Feauveau 1.1 with 9.7 and B-spline 3. The number of used carriers is 128, 512, and 1,024. Quadrature phase shift key (QPSK) is used with cyclic prefix 1/16 and a bandwidth of 20 MHz. traditional fast fourier transform (FFT) system is compared to the proposed discrete wavelet packet transform (DWPT) to show the BER enhancements. The space-time block coding (STBC) is used to enhance system cabability in error corection. The proposed system shows significant improvement in BER, so that, it reaches to the same BER when using FFT but with less signal to noise ratio (SNR), which interns reduce the power consumed within the system and the cost.

This is an open access article under the [CC BY-SA](#) license.



Corresponding Author:

Osama Qasim Jumah Al-Thahab

Department of Electrical, College of Engineering, University of Babylon

Hillah, Babil, Iraq

Email: eng.osama.qasim@uobabylon.edu.iq

1. INTRODUCTION

The recent advancements in data network gave rise to many applications that are involved with almost every aspect of life ranging from top secret military operation to merely sending greetings for a birthday [1], [2]. These networks are becoming the backbone of societies because people are relying on them to spread news all over the world [3]–[5]. Even the elections consider social networks as a reliable source of information to study the citizen's point of views regarding a certain party or a candidate. Presently, these networks are growing to be self-sustained economic systems and a pillar of modern societies [6], [7].

To satisfy the higher bandwidths, the engineers could follow the traditional way by providing the extra bandwidths for the networks. Although this might be satisfactory it suffers from by unavoidable limitations. First limitation is the scares affordable free bandwidth because the radio frequency (RF) spectrum is highly congested. The second limitation is the bandwidth over a wide range will increase the influence of nonlinearity and deformations effect on the transmitted signals [8]–[11]. Differnt approaches will invented to modulate the data that used narrower bandwidth with higher data rates, like the multi-carrier transmission (MC) or its modern version the orthogonal frequency division multiplexing (OFDM) [12], [13].

Khan *et al.* [14] suggested a system of using discrete wavelet packet transform (DWPT) in OFDM instead of discrete fourier transform (DFT), then compared the performance between them based on bit error rate (BER) values and their corresponding signal to noise ratio (SNR), while Soni *et al.* [15], used a discrete wavelet transform (DWT) instead of fast fourier transform (FFT) in the OFDM system and test the proposed system by sending various images through different channels. They found that, the DWT is more reliable and has less SNR as compared to FFT. The use of these techniques is very important in many application as Roy *et al.* [16] depicts in his paper, so that a comparison is made between the FFT, discrete cosine transform (DCT), DWT and wals-hadamard transform (WHT) in many applications like electrocardiogram and photo-plethysmography signals. This paper aims to improve the BER of the code division multiple access (CDMA) multicarrier system by adding a DWPT instead of FFT as a suggestion to the system. Here the effected thing is reducing the SNR of the proposed system so that it reaches to the same BER but with low power, which consequently reduce the complexity and cost.

2. MC AND OFDM SYSTEMS

The idea of OFDM is based on dividing high bit rate stream of data into low bit stream segments. These segments are then modulated using orthogonal subcarriers to ensure neither overlapping between adjacent. These sub-streams are then combined together and transmitted using a main carrier before transmission. The block diagram of typical OFDM system is shown in Figure 1. Due to the fact that the resultant subs-terms have low rate with a low bandwidth requirement, then the OFDM requires less channel compared with the classical system. The fact that the subcarriers are orthogonal also allows the channels to overlap without interference because the orthogonality ensures complete separation among channels [12]. The carriers and pilots illustration are shown in Figure 2, so that, Figure 2(a) depicts the user and pilot subcarriers and how the packets are performed, while Figure 2(b) states the effect of orthogonality on the subcarrier [13].

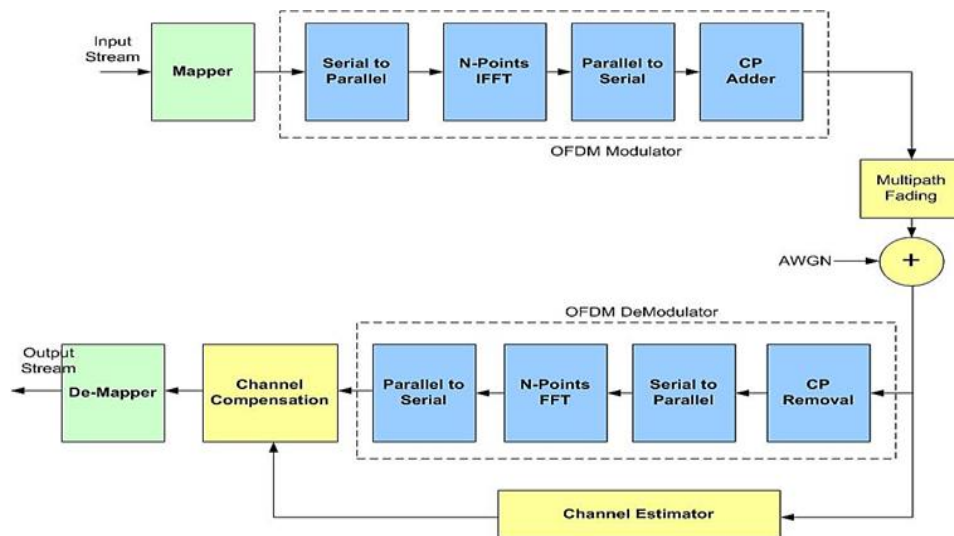


Figure 1. OFDM block diagram

Consider a multi-carrier (MC) OFDM system with N subcarriers and each subcarrier f_k is used to modulate s_k sub-frame, then $s(t)$ transmitted signal is (1):

$$s(t) = \sum_{k=1}^N s_k \exp(j2\pi k f_k t) \quad (1)$$

Here f_k is equally spaced subcarriers and $f_k = BW/N$, BW is the bandwidth.

Let T to be $2/BW$, then according to Nyquist theorem each sample occurs at $T/2$ or $1/BW$. Therefore, any sub-stream subcarrier will exist at time mT then (1) becomes:

$$s(mT) = \sum_{k=1}^N s_k \exp\left(j2\pi \frac{km}{N}\right) \quad (2)$$

In (2) is exactly the inverse discrete fourier transform (IDFT) or inverse fast fourier transform (IFFT). At the receiver, an FFT circuit can be used to retrieve the transmitted signals from the incoming samples. This is quite clear from Figure 1, where the symbols are modulated, possibly using quadrature amplitude modulation (QAM) [13].

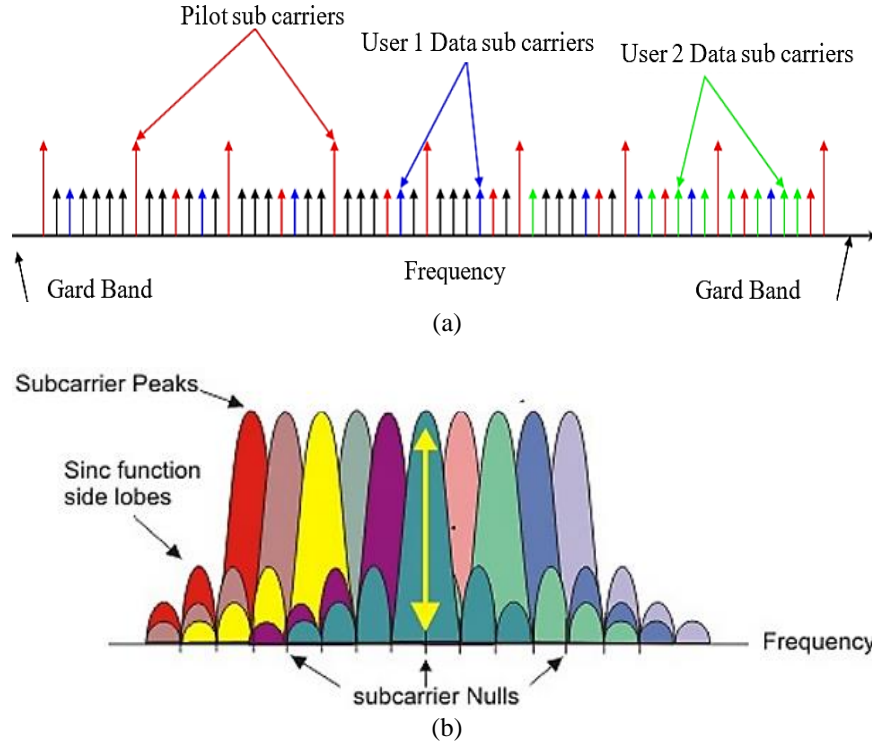


Figure 2. OFDM idea; (a) the subcarriers assignment to users with pilot carriers and (b) OFDM signal spectrum

3. DISCRETE WAVELET PACKET TRANSFORM DWPT

In (2) can be viewed as a running filter with coefficients $\exp\left(j2\pi\frac{km}{N}\right)$ or in other words a low pass filter bank. The frequency location for each subcarrier f_k occurs at every $2^k \times f_0$, where f_0 is the fundamental frequency and f_k are its harmonics. This means that the power spectral density (PSD) will be widely spread over the channel as the sinusoidal functions extends from $-\infty$ to $+\infty$. This consequently reduces the system spectral efficiency. In order to solve this problem, the analyzing function $\exp\left(j2\pi\frac{km}{N}\right)$ can be replaced by a more compact or spectral efficient function to ensure higher PSD concentration [14]. The DWT can ensure the achievement of this goal. Hence; by replacing DFT or FFT with DWT, the spectral efficiency can be increased due to time limited period of DWT functions resulting in a more reliable and higher signal quality [15], [16]. The wavelets are orthonormal functions such that [17], [18]:

$$\langle \Psi_l(t), \Psi_k(t) \rangle = \int \Psi_l(t) \Psi_k(t) dt = \begin{cases} 1 & l = k \\ 0 & l \neq k \end{cases} \quad (3)$$

Where $\Psi(t)$ is the mother wavelet, and $\langle \cdot \rangle$ is inner product. The p vanishing moments can be found as (4):

$$\int_{-\infty}^{\infty} t^k \Psi(t) dt = 0 \text{ for } 0 \leq k < p \quad (4)$$

The vanishing moments describe the speed of decay of the wavelet function. So, the DWT output is:

$$X_\Psi(s, r) = \int_{-\infty}^{\infty} x(t) \Psi_{t,r}(t) dt \quad (5)$$

Where s, r is the scale and translation. This means that the wavelet can capture the details of $x(t)$ in both time and frequency unlike FFT, which focuses only on the frequency domain. The translation means the wavelet is shifted in time while the scale is related to the width of the finite wavelet function. The scale and translation are shown in Figure 3 [19]. Assume an S samples discrete signal $x[n]$ ($n = 0, 1, \dots, S-1$) want to apply first level DWT to it, then:

$$y[n] = \sum_{k=-\infty}^{\infty} x[k]G_0[2n-k] + \sum_{k=-\infty}^{\infty} x[k]G_1[2n-k] = y_{low}[n] + y_{high}[n] \quad (6)$$

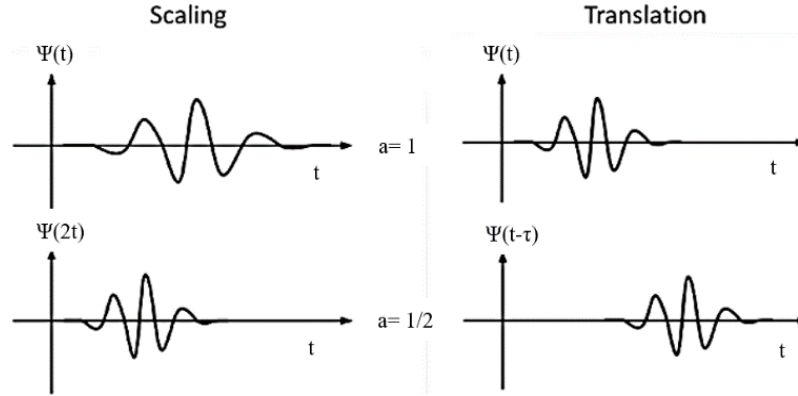


Figure 3. The scale and translation of wavelet

In (6), the y_{low} is the signal coming from the low pass filter (LPF) bank with its impulse response $G_0[2n-k]$, while, y_{high} is the signal coming from the high pass filter (HPF) bank with its impulse response $G_1[2n-k]$. It is noted that the out coming signal has double the sampling rate n as the input signal. Thus, a decimation circuit by 2 ($\downarrow 2$) is required to switch back to the original sampling rate. Figure 4 shows the filter bank of the multi-level DWT [20]. The DWT functions G_0 and G_1 suggest that the incoming signal will be transformed to orthogonal frequencies in the rate of $\frac{f}{2^k}$ where $k = 1, 2, \dots, K$ which is the number of analysis levels. The reconstruction functions H_0 and H_1 are the inverse for the analyzing functions G_0 and G_1 . In reconstruction filter, the sampling rate is up by a factor of 2 ($\uparrow 2$) to reverse the decimation process. The DWT can be modified to be identical to FFT and further increases the final signal PSD concentration. The modification comes from decomposing y_{high}^1 in the same manner y_{low}^1 at every stage. This analysis is called DWPT. The filters used for DWPT is shown in Figure 5 [21], [22].

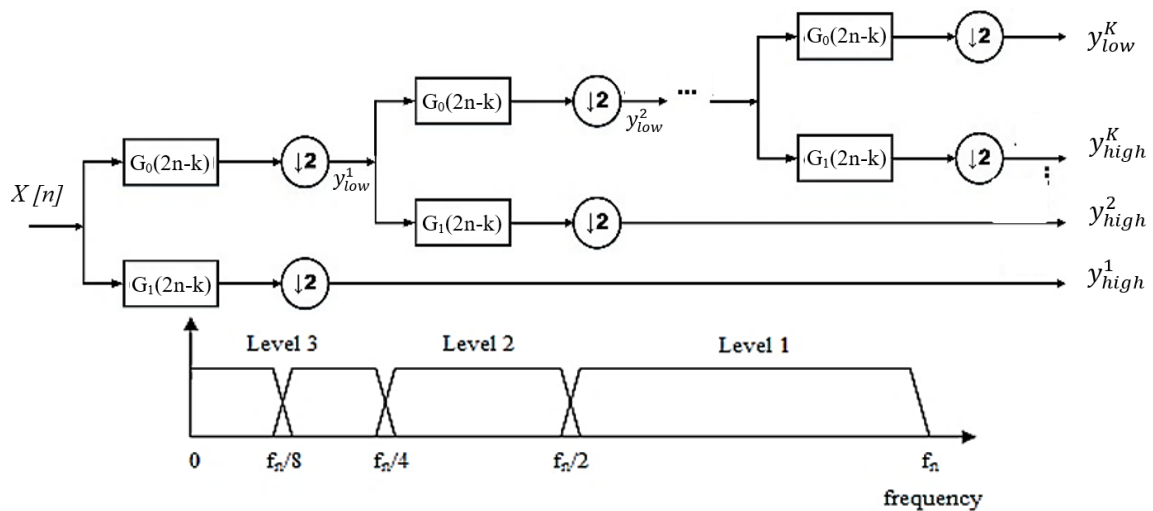


Figure 4. Filter banks and LPF response

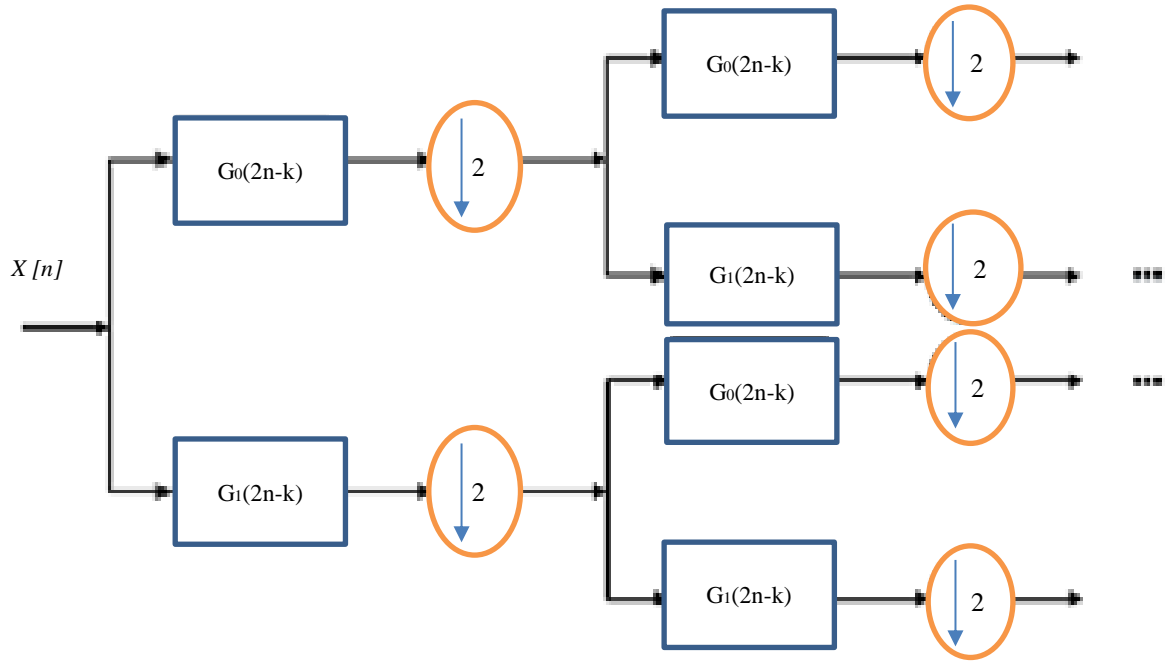


Figure 5. DWPT analysis filter

To generate the orthonormal subcarriers by using inverse discrete wavelet packet transform (IDWPT), consider (6) and by using mallat's pyramid algorithm (MPA) for multi-resolution analysis (MRA), in (6) can be written as (7), so that $g(k)$ is called the wavelet coefficient function and is related to $h(\cdot)$ (10). Then for a scaling function of order N , in (11) can be depicted. In addition, the dilation and wavelet equations can be written as seen in (12) and (13):

$$y(t) = \sum_{k=-\infty}^{\infty} a_{j_0}(k) \Phi_{j_0}(t - k) + \sum_{j=j_0}^{\infty} \sum_{k=-\infty}^{\infty} b_j(k) \Psi_j(2^m t - k) \quad (7)$$

$$a_j(k) = \sum_m h(m - 2k) a_{j+1}(m) \quad (8)$$

$$b_j(k) = \sum_m g(m - 2k) b_{j+1}(m) \quad (9)$$

$$g(k) = (-1)^k h(1 - k) \quad (10)$$

$$g(k) = (-1)^k h(N - 1 - k) \quad (11)$$

$$\Phi(t) = \sqrt{2} \sum_{k=0}^{N-1} h(k) \Phi(2t - k) \quad (12)$$

$$\Psi(t) = \sum_{k=0}^{N-1} (-1)^k h(k) \Phi(2t + k - N + 1) \quad (13)$$

Therefore, by using MPA and extending it to the DWPT, series of $x[n]$ vector can be analyzed using the following transformation matrix for L number of stages [23], [24].

$$\mathbf{A} = \begin{bmatrix} h(0) & h(1) & h(2) & h(3) & \cdots & h(L-1) & 0 & 0 & \cdots & 0 & 0 \\ 0 & 0 & h(0) & h(1) & h(2) & h(3) & \cdots & h(L-1) & 0 & \cdots & 0 \\ \vdots & \vdots & \vdots & \vdots & \vdots & \vdots & \vdots & \vdots & \vdots & \vdots & \vdots \\ h(4) & \cdots & h(L-1) & 0 & 0 & \cdots & 0 & h(0) & h(1) & h(2) & h(3) \\ h(2) & h(3) & \cdots & h(L-1) & 0 & 0 & \cdots & 0 & 0 & h(0) & h(1) \\ g(0) & g(1) & g(2) & g(3) & \cdots & g(L-1) & 0 & 0 & \cdots & 0 & 0 \\ 0 & 0 & g(0) & g(1) & g(2) & g(3) & \cdots & g(L-1) & 0 & \cdots & 0 \\ \vdots & \vdots & \vdots & \vdots & \vdots & \vdots & \vdots & \vdots & \vdots & \vdots & \vdots \\ g(4) & \cdots & g(0) & 0 & \cdots & 0 & 0 & g(0) & g(1) & g(2) & g(3) \\ g(2) & g(3) & \cdots & g(L-1) & 0 & 0 & \cdots & 0 & 0 & g(0) & g(1) \end{bmatrix} \quad (14)$$

By substituting (11) in (14), the transformation matrix becomes:

$$A = \begin{bmatrix} h(0) & h(1) & h(2) & h(3) & \dots & h(L-1) & 0 & 0 & \dots & 0 & 0 \\ 0 & 0 & h(0) & h(1) & h(2) & h(3) & \dots & h(L-1) & 0 & \dots & 0 \\ \vdots & \vdots & \vdots & \vdots & \vdots & \vdots & \vdots & \vdots & \vdots & \vdots & \vdots \\ h(4) & \dots & h(L-1) & 0 & \dots & 0 & 0 & h(0) & h(1) & h(2) & h(3) \\ h(2) & h(3) & \dots & h(L-1) & 0 & 0 & \dots & 0 & 0 & h(0) & h(1) \\ h(L-1) & -h(L-2) & h(L-3) & \dots & h(1) & -h(0) & 0 & 0 & \dots & 0 & 0 \\ 0 & 0 & h(L-1) & -h(L-2) & h(L-3) & \dots & h(1) & -h(0) & 0 & \dots & 0 \\ \vdots & \vdots & \vdots & \vdots & \vdots & \vdots & \vdots & \vdots & \vdots & \vdots & \vdots \\ h(L-5) & \dots & h(0) & 0 & \dots & 0 & 0 & h(L-1) & -h(L-2) & h(L-3) & -h(L-4) \\ h(L-3) & \dots & h(1) & -h(0) & 0 & 0 & \dots & 0 & 0 & h(L-1) & -h(L-2) \end{bmatrix} \quad (15)$$

Using the orthonormal property, the reconstruction matrix is simply the transpose of the analysis function. Hence, at the construction side the following matrix is used (16):

$$C = \begin{bmatrix} h(0) & 0 & 0 & \dots & 0 & 0 & h(2) & h(L-1) & 0 & 0 & 0 & h(1) \\ h(1) & 0 & 0 & \dots & 0 & 0 & \vdots & \vdots & 0 & 0 & 0 & -h(0) \\ \vdots & h(0) & 0 & \dots & 0 & 0 & h(L-1) & h(1) & h(L-1) & 0 & 0 & 0 \\ h(L-1) & h(1) & 0 & \dots & 0 & 0 & 0 & -h(0) & \vdots & 0 & 0 & 0 \\ 0 & \vdots & h(0) & \dots & \vdots & 0 & 0 & 0 & h(1) & h(1) & \vdots & 0 \\ 0 & h(L-1) & h(1) & \dots & 0 & 0 & 0 & 0 & -h(0) & \vdots & 0 & 0 \\ 0 & 0 & \vdots & \dots & 0 & \vdots & 0 & 0 & 0 & -h(1) & 0 & \vdots \\ 0 & 0 & h(L-1) & \dots & 0 & 0 & 0 & 0 & 0 & h(0) & 0 & 0 \\ 0 & 0 & 0 & \dots & 0 & 0 & 0 & 0 & 0 & 0 & 0 & 0 \\ \vdots & 0 & 0 & \dots & 0 & 0 & \vdots & 0 & 0 & 0 & 0 & 0 \\ 0 & \vdots & 0 & \dots & h(0) & 0 & \vdots & 0 & \vdots & 0 & h(L-1) & 0 \\ 0 & 0 & \vdots & \dots & h(1) & 0 & 0 & 0 & 0 & \vdots & \vdots & h(L-1) \\ 0 & 0 & 0 & \dots & \vdots & h(0) & 0 & 0 & 0 & 0 & -h(1) & \vdots \\ 0 & 0 & 0 & \dots & h(L-1) & h(1) & 0 & 0 & 0 & 0 & h(0) & h(2) \end{bmatrix} \quad (16)$$

4. OFDM AND CDMA SYSTEMS

The OFDM can ensure a complete separation for overlapped channels due to the orthogonality property. This property is tightly adhered to the location of subcarriers. If the location of these subcarriers are dispositioned, then the orthogonality will fall apart and the system will experience the inter channel interference (ICI) [24]. The ICI will reduce the system performance due to the decrease in the signal quality. Therefore, certain modifications should be taken, and one of them is using CDMA [25]. The CDMA is built upon the spread spectrum system (SSS) technology by which it allows all the users to use the channel all the time. A typical CDMA is shown in Figure 6 [26]. In the CDMA, each user is assigned by a pseudo noise-sequence (PN-sequence). The word pseudo comes from the fact that the sequence will repeat itself after a period of time depending on the linear feedback shift register (LFSR) constraint length. The generated PN pulses are almost random. The auto correlation function (ACF) of the PN sequence has the property given in (17) [27].

$$ACF(t) = \int PN(t)PN(t+\tau)d\tau = \begin{cases} 1 & \tau = 0 \\ -\frac{1}{N} & \tau \neq 0 \end{cases} \quad (17)$$

Where N is the maximal length and equals to 2^n-1 and n is the LFSR constraint length.

When the PN sequence is aligned with itself then the ACF will have 1 value otherwise the sequence will cancel the incoming data. Unfortunately, the PN-sequence has poor cross correlation function (CCF), so gold code is used. If the sequences are chosen carefully, then the CCF will have only three states, which are:

$$\left\{ \frac{-t(n)}{N}, -\frac{1}{N}, \frac{t(n)-2}{N} \right\} t(n) = \begin{cases} 1 + 2^{\frac{n+1}{2}} & \text{for } n \text{ odd} \\ 1 + 2^{\frac{n+2}{2}} & \text{for } n \text{ even} \end{cases} \quad (18)$$

At the receiver side, the incoming streams are multiplied by the same gold code, then passed through a coherent detector as seen in Figure 7 [26]–[28]. Let the transmitted OFDM signal to be $s(t)$, then the received signal $y(t)$ is seen in (19):

$$y(t) = s(t)\check{c}(t) + N(t) \quad (19)$$

where $\check{c}(t)$ is the spreading code at the transmitter side, $N(t)$ is the impairments from the channel like noise or jamming or interference or multipath.

$$N(t) = n(t) + J(t) + \sum_{i=1}^M s(t - \tau_i) \check{c}(t - \tau_i) \quad (20)$$

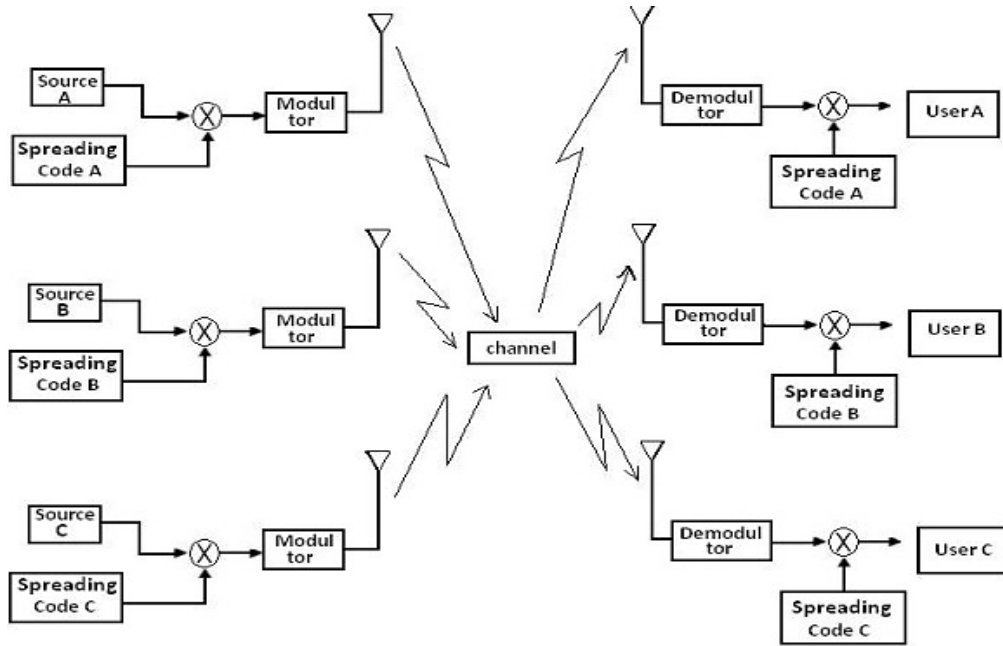


Figure 6. A typical CDMA system block diagram

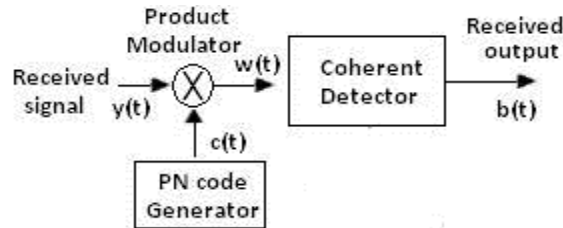


Figure 7. A detailed spread spectrum demodulator

Where $n(t)$ is the additive wide gaussian noise (AWGN), $J(t)$ is the jamming signal, τ is the time delay due to multipath and M is the number of multipath signals. After multiplying $y(t)$ by $c(t)$ then output signal $b(t)$ of the coherent detector for the input $s(t)$ is:

$$b(t) = \frac{1}{T_s} \left[\int_0^{T_s} s(t) \check{c}(t) c(t) dt + \int_0^{T_s} N(t) c(t) dt \right] \quad (21)$$

5. FREQUENCY FLAT FADING CHANNEL AND SPACE TIME BLOCK CODING

The practical channels are usually imperfect and thus are described using its impulse response. assume a frequency selective fading channel is h of length L then the received signal $r(t)$ is given in (22) [29]:

$$r(n) = \sum_{k=0}^{L-1} h(k) s(n - k) \quad (22)$$

Where $s(n)$ is the transmitted signal, in (22) shows that the channel with such channel impulse response (CIR) which will cause inter-symbols interference (ISI) or in the case of OFDM will be worse which is inter-block interference (IBI) or ICI. One of the methods that used to overcome the fading effect is the multiple-input and multiple-output (MIMO)-space time block coding (STBC) [30]. MIMO is a technique by which the symbol is transmitted through different paths in order to null the CIR. Here Alamouti's STBC is used to avoid the continuous need to update the CIR [31].

The simplest form of Alamouti scheme is the multiple-input single-output (MISO) of 1×2 which means that the number of receiving antennas is 1 and the transmitting antennas is 2 as in Figure 8. Let two symbols x_1 and x_2 to be transmitted by this MISO over two channels of CIR or sometimes called channel state information (CSI) of h_1 and h_2 , then the received symbols are:

$$y_1(t) = [h_1 \ h_2] \begin{bmatrix} x_1 \\ x_2 \end{bmatrix} + n_1(t) \quad (23)$$

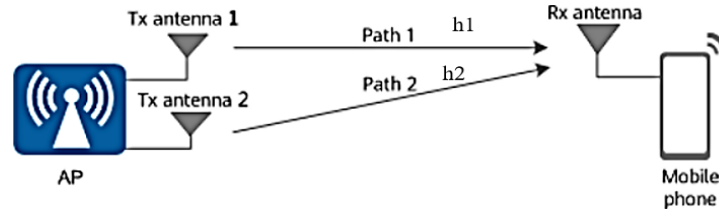


Figure 8. A 2×1 single input multiple output (SIMO) system

At the second instance, the first antenna will transmit $x_2^*(t)$ and the second antenna will transmit $-x_1^*(t)$, so the received symbols at the second instance are:

$$y_2(t) = [h_1 \ h_2] \begin{bmatrix} x_2^* \\ -x_1^* \end{bmatrix} + n_2(t) \quad (24)$$

Taking the conjugate of (24) and arranging the result to look like:

$$y_2^*(t) = [-h_2^* \ h_1^*] \begin{bmatrix} x_1 \\ x_2 \end{bmatrix} + n_2^*(t) \quad (25)$$

Where $n_1(t)$ and $n_2(t)$ are the AWGN in the first and second transmission instances respectively. Combining (24) with (25), then it can be shown that:

$$\begin{bmatrix} y_1(t) \\ y_2^*(t) \end{bmatrix} = \begin{bmatrix} h_1 & h_2 \\ -h_2^* & h_1^* \end{bmatrix} \begin{bmatrix} x_1(t) \\ x_2(t) \end{bmatrix} + \begin{bmatrix} n_1(t) \\ n_2^*(t) \end{bmatrix} \quad (26)$$

$$\text{Let } Y = \begin{bmatrix} y_1(t) \\ y_2^*(t) \end{bmatrix}, C_1 = \begin{bmatrix} h_1 \\ -h_2^* \end{bmatrix}, C_2 = \begin{bmatrix} h_2 \\ h_1^* \end{bmatrix} \text{ and } N = \begin{bmatrix} n_1(t) \\ n_2^*(t) \end{bmatrix} \text{ then } Y = [C_1 \ C_2] \begin{bmatrix} x_1(t) \\ x_2(t) \end{bmatrix} + N$$

Here, the Alamouti orthogonal space time block code (OSTBC) can be extended from MISO to MIMO easily [32], [33]. H_1 and H_3 is depicted in (27) and so on for H_4 .

$$H_1 = \begin{bmatrix} h_1 & h_2 \\ -h_2^* & h_1^* \end{bmatrix} \text{ and } H_3 = \begin{bmatrix} H_1 & H_2 \\ -H_2^* & H_1^* \end{bmatrix} \quad (27)$$

6. RESULTS AND DISCUSSION

The suggested system combines all the above concepts and integrate them into a single communication system as shown in Figure 9. First, the signals are mapped using quadrature phase shift key (QPSK) scheme. An OSTBC is added then the resultant stream is fed to IDWPT section to generate the orthogonal subcarriers. These pilots are used for synchronization and estimating the CSI of the channel in order to provide the necessary equalization if needed. This serial stream is then fed to a MIMO of 2×2 antennas then send over the channel.

The transmitter is assumed to be a mobile travelling at speeds 2 km/hr, 45 km/hr, and 100 km/hr creating maximum doppler shift (MDS) of 10.7 Hz, 241.7 Hz, and 537 Hz respectively. The channel is flat fading rayleigh channel with AWGN. The number of transmitted bits per test is (102,400 bits) coming from (100 packet*64 characters *16 bit/char). The OFDM physical layer settings are shown in Table 1.

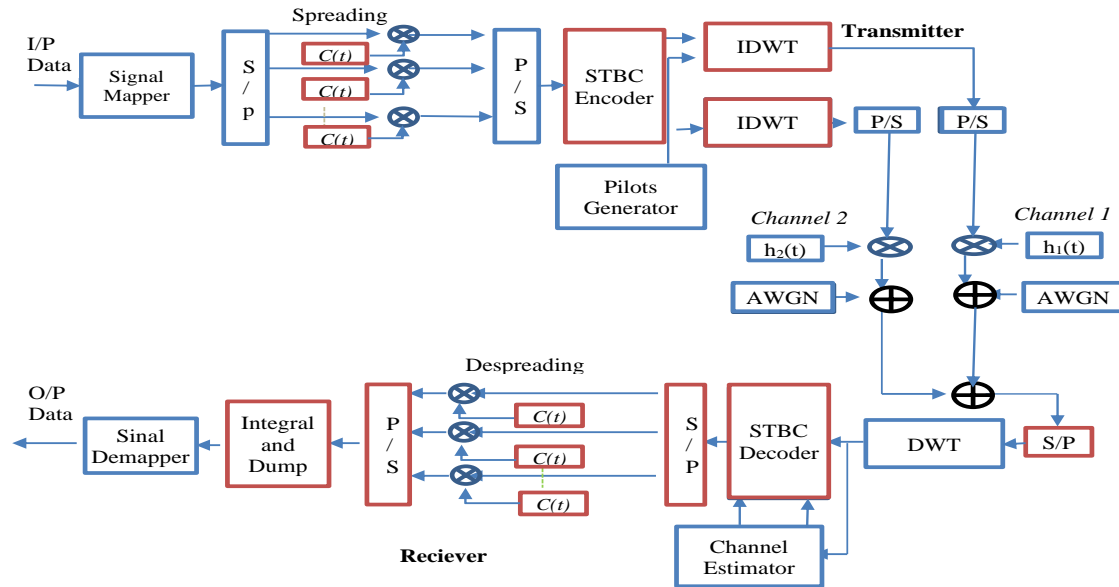


Figure 9. The complete suggested communication system

Table 1. OFDM physical layer simulation settings

Parameter	Mobile MC-DS-CDMA Scalable OFDMA-PHY			
FFT or DWT size	128	512	1024	2048
Number of used data subcarriers	64	180	360	720
Modulation types	QPSK			
Cyclic prefix	1/16			
Channel bandwidth (MHz)	20	20	20	20

Here, the mother wavelets utilized are as follows: Haar, Daubechies=db4, Symlets=sym4, Cohen-Daubechies-Feauveau=cdf, and B-spline 3=bs3. The results are as follows:

- MDS 10.7 Hz, the BER are shown in Figure 10 (see in Appendix)
- MDS 241.7 Hz, the BER are shown in Figure 11 (see in Appendix)
- MDS 537 Hz, the BER are shown in Figure 12 (see in Appendix)

From Figure 10, it can be seen that to obtain a 10^{-3} BER, the SNR must be at least 28 dB, while by using the proposed system it decreased to about 5 dB when using 512 subcarriers, and so on for the others. The percentage improvement is about 80 percent, which is very good. The big difference between the results of the proposed system and the traditional method beyond to the excellent orthogonality of DWPT over FFT, which reduces the effect of ICI and ISI on the transmitted data.

A comparison is made when motor driven systems (MDS) equal to 10.7 Hz [30], they reach to 10^{-3} BER (128 subcarrier) at 8 dB SNR in AWGN, while the proposed system reaches the same value at 5 dB. In addition, Ali *et al.* [34] for the same sub carrier reaches to 7 dB SNR, while at 1,024 subcarriers the SNR is 8 dB and the proposed system of this work gives 7 dB. In the same context, Kusumawardhanian *et al.* [35] obtain SNR of about 7.5 dB over AWGN channel when using a multi-level coding CDMA. This comparison gives the preference of the proposed system over different algorithms used to enhance the BER evaluation.

7. CONCLUSION

Here, IDWPT/DWPT has an excellent performance as compared to the IFFT/FFT in all tests. This justifies the assumption that the DWPT has higher concentrated signal PSD. But in all cases, the BER increases with the increase of bit rate and this event is inevitable. The doppler shift has high impact on system performance as it increases due to the motion of the mobile station. The doppler shift changes the locations of the orthogonal subcarriers which derails the orthogonality that depends on the difference between adjacent subcarriers, although, the pilots were transmitted to resynchronize the system but even at certain bit rate and motion speed they lose their effectiveness. Neither the STBC nor the CDMA are now able to track and fight of the doppler shift effect. It is highly noticed that the wavelets have no close relation to the bit rate and inspite of that, there are some kinds of wavelets that gives the worst performance upon FFT like bs3. Therefore, the wavelet selection should be carefully done.

APPENDIX

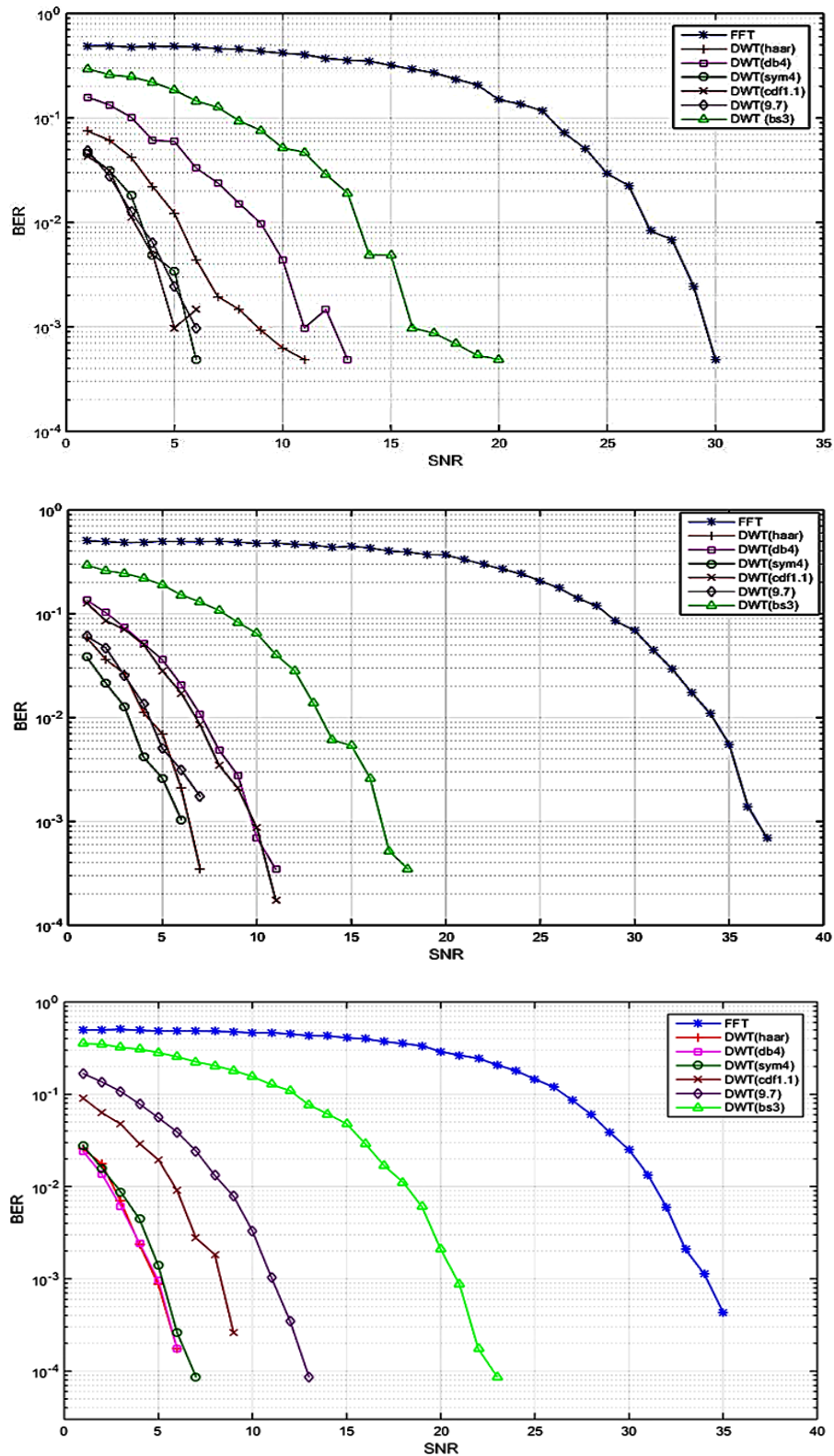


Figure 10. BER performance of STBC DWT-mobile MC-DS-CDMA in AWGN-flat fading channel with 128, 512, and 1,024 subcarriers respectively

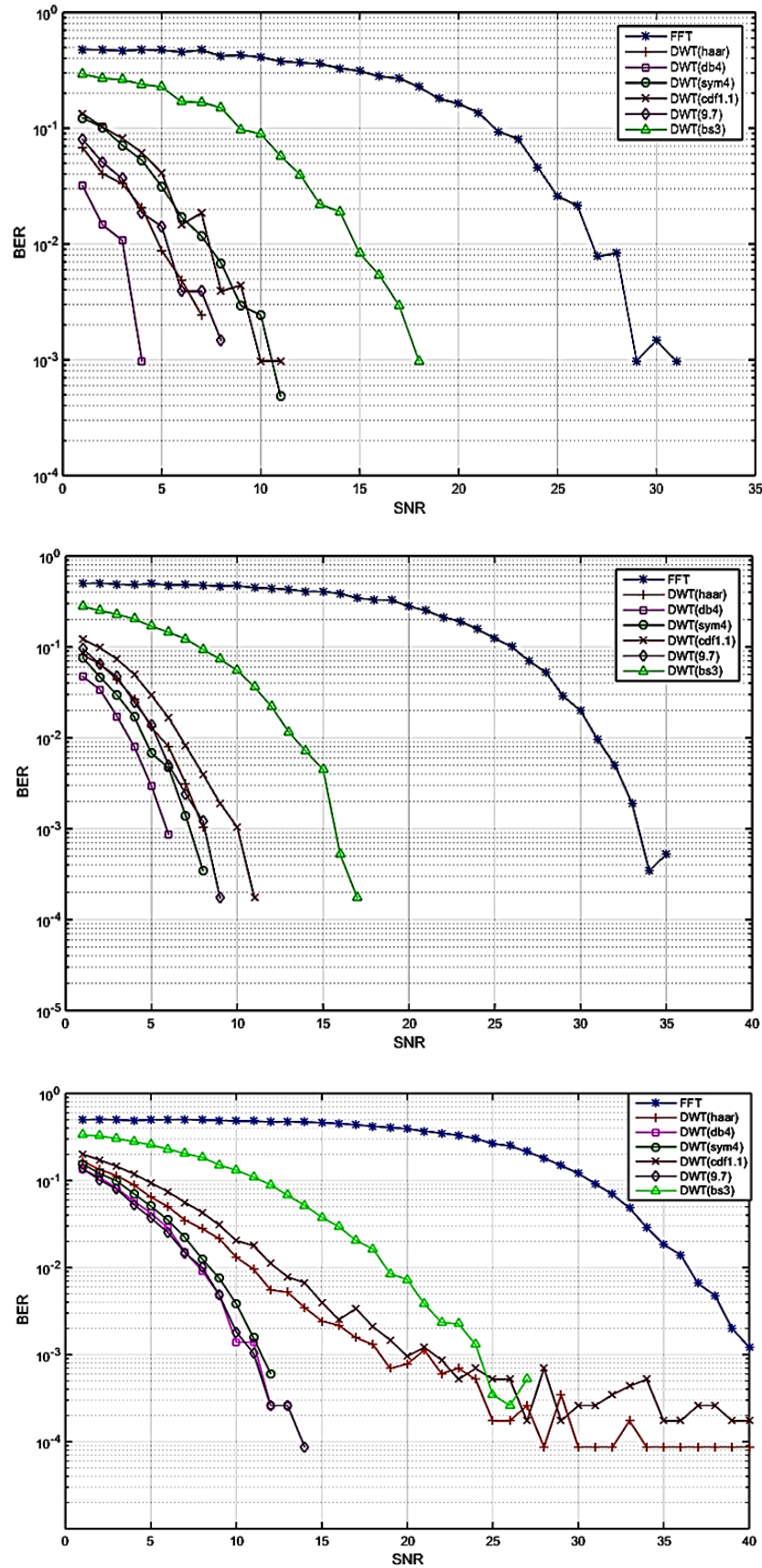


Figure 11. BER performance of STBC DWT-mobile MC-DS-CDMA in AWGN-flat channel with 128, 512, and 1,024 subcarriers respectively

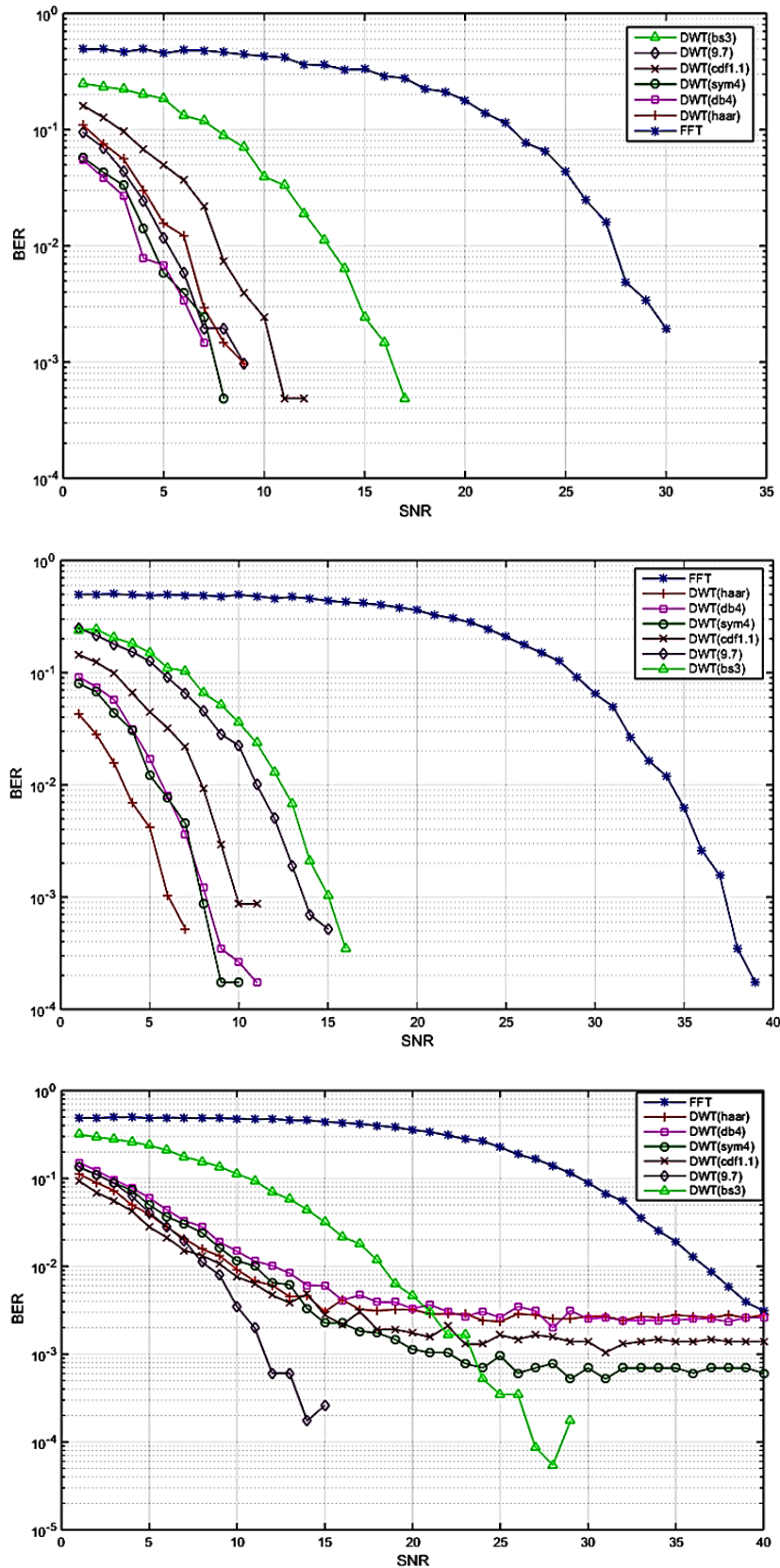


Figure 12. BER performance of STBC DWT-mobile MC-DS-CDMA in AWGN-flat channel with 128, 512, and 1,024 subcarriers respectively




REFERENCES

- [1] K. Moskvitch, "Securing IoT: In your smart home and your connected enterprise," *Engineering and Technology*, vol. 12, no. 3, pp. 40–42, 2017, doi: 10.1049/et.2017.0303.
- [2] D. Sewwandi, K. Perera, S. Sandaruwan, O. Lakchani, A. Nugaliyadde, and S. Thelijjagoda, "Linguistic features based personality recognition using social media data," in *2017 6th National Conference on Technology and Management (NCTM)*, Jan. 2017, pp. 63–68, doi: 10.1109/NCTM.2017.7872829.
- [3] S. I. Khan and A. S. M. L. Hoque, "Health data integration with Secured Record Linkage: A practical solution for Bangladesh and other developing countries," in *2017 International Conference on Networking, Systems and Security (NSysS)*, Jan. 2017, pp. 156–161, doi: 10.1109/NSysS.2017.7885818.
- [4] C. C. Mawele and R. Pellissier, "A framework for the development of management skills for co-operative development in an agri-business value chain in South Africa," in *2016 Portland International Conference on Management of Engineering and Technology (PICMET)*, Sep. 2016, pp. 1429–1441, doi: 10.1109/PICMET.2016.7806703.
- [5] D. Kaur and D. Garg, "Variable bid fee: An online auction shill bidding prevention methodology," in *2015 IEEE International Advance Computing Conference (IACC)*, Jun. 2015, pp. 381–386, doi: 10.1109/IADCC.2015.7154735.
- [6] M. Pouryazdan, B. Kantarci, T. Soyata, L. Foschini, and H. Song, "Quantifying User Reputation Scores, Data Trustworthiness, and User Incentives in Mobile Crowd-Sensing," *IEEE Access*, vol. 5, pp. 1382–1397, 2017, doi: 10.1109/ACCESS.2017.2660461.
- [7] S. Shi, D. Jin, and G. Tiong-Thye, "Real-time Public Mood Tracking of Chinese Microblog Streams with Complex Event Processing," *IEEE Access*, vol. 5, pp. 421–431, 2017, doi: 10.1109/ACCESS.2016.2633721.
- [8] S. Wicha, T. Photiphun, P. Janjaroenpan, C. Taweesak, I. Chainilwan, and P. Rodmanee, "Proposed of e-Community Supported Agriculture (e-CSA) system to promote local organic products: The empirical study of Chiang Rai province," in *2017 International Conference on Digital Arts, Media and Technology (ICDAMT)*, 2017, pp. 273–281, doi: 10.1109/ICDAMT.2017.7904976.
- [9] X. Chen, S. Peng, J. Z. Huang, F. Nie, and Y. Ming, "Local PurTree Spectral Clustering for Massive Customer Transaction Data," *IEEE Intelligent Systems*, vol. 32, no. 2, pp. 37–44, Mar. 2017, doi: 10.1109/MIS.2017.41.
- [10] P. Kaur, M. Goyal, and J. Lu, "A Comparison of Bidding Strategies for Online Auctions Using Fuzzy Reasoning and Negotiation Decision Functions," *IEEE Transactions on Fuzzy Systems*, vol. 25, no. 2, pp. 425–438, Apr. 2017, doi: 10.1109/TFUZZ.2016.2598297.
- [11] S. A. K. G. Samaraweera, N. G. H. P. Gamage, I. G. Gallage, D. D. T. M. Gunathilaka, N. Fernando, and D. Kasthurirathna, "A trilateral influence model for online shopping," in *2017 6th National Conference on Technology and Management (NCTM)*, Jan. 2017, pp. 75–80, doi: 10.1109/NCTM.2017.7872831.
- [12] H. Schulze and C. Lüders, *Theory and Applications of OFDM and CDMA: Wideband Wireless Communications*. Germany: Wiley, 2006, doi: 10.1002/0470017406.
- [13] R. Van Nee and R. Prasad, *OFDM for Wireless Multimedia Communications (Artech House Universal Personal Communications)*, vol. 3. London: Artech House Publishers, 2000.
- [14] A. Khan, M. R. Usman, M. B. Shahab, and S. Y. Shin, "Performance comparison of DFT and DWPT based OFDM system using 64 DAPSK," in *2016 International Conference on Smart Green Technology in Electrical and Information Systems (ICSGTEIS)*, Oct. 2016, pp. 59–63, doi: 10.1109/ICSGTEIS.2016.7885767.
- [15] A. Soni, S. J. Basha, and A. C. Tiwari, "Comparative Analysis of OFDM under FFT and DWT Based Image Transmission," *International Journal of Innovative Research in Computer and Communication Engineering*, vol. 1, no. 2, pp. 371–378, 2013.
- [16] A. B. Roy, D. Banerjee, and A. Professor, "Comparison of FFT, DCT, DWT, WHT Compression Techniques on Electrocardiogram & Photoplethysmography Signals," in *Special Issue of International Journal of Computer Applications*, 2012, pp. 975–9887.
- [17] H. Olkkonen, *Discrete Wavelet Transforms - Algorithms and Applications*. Finland: IntechOpen, 2012, doi: 10.5772/817.
- [18] M. V. Wickerhauser, *Adapted Wavelet Analysis from Theory to Software*, London: CRC Press, vol. 38, no. 1, 1996.
- [19] L. Debnath and F. A. Shah, *Wavelet transforms and their applications*, 2nd ed., vol. 48, no. 1. USA: Birkhäuser Boston, MA, 2003, doi: 10.5860/choice.39-6472.
- [20] H. Raouf, H. Yousef, and A. Ghonem, "An Analytical Comparison between Applying FFT and DWT in WiMAX Systems," *IJCSI International Journal of Computer Science Issues*, vol. 11, no. 6, pp. 18–26, 2014.
- [21] H. de O. Mota, F. H. Vasconcelos, and R. M. da Silva, "Real-time wavelet transform algorithms for the processing of continuous streams of data," in *IEEE International Workshop on Intelligent Signal Processing*, 2005., 2005, pp. 346–351, doi: 10.1109/WISP.2005.1531683.
- [22] D. B. Percival and A. T. Walden, *Wavelet Methods for Time Series Analysis*. London: Cambridge University Press, 2000, doi: 10.1198/jasa.2002.s460.
- [23] S. G. Mallat, "Multiresolution approximations and wavelet orthonormal bases of $L_2(\mathbb{R})$," *Transactions of the American mathematical society*, vol. 315, no. 1, pp. 69–87, 1989.
- [24] I. Mehmood, M. A. Ashraf, and K. Shabir, "Capacity enhancement using adaptive power and sub-carriers allocation under imperfect CSI in MC-CDMA systems," in *Proceedings of 2017 14th International Bhurban Conference on Applied Sciences and Technology, IBCAST 2017*, 2017, pp. 782–786, doi: 10.1109/IBCAST.2017.7868143.
- [25] D. V. Gayvoronskiy and E. A. Danilchuk, "Analysis of multiple-access interference for CDMA signals," in *2017 IEEE Conference of Russian Young Researchers in Electrical and Electronic Engineering (EIconRus)*, 2017, pp. 144–145, doi: 10.1109/EIconRus.2017.7910514.
- [26] M. K. Simon *et al.*, *Spread Spectrum Communications Handbook*. USA: The McGraw-Hill Companies, Inc., 2002.
- [27] J. S. Lee and L. E. Miller, *CDMA systems engineering handbook*. London: Artech House, 1998.
- [28] M. A. Abu-Rgheff, *Introduction to CDMA Wireless Communications*. USA: Elsevier, 2007, doi: 10.1016/B978-0-7506-5252-0.X5001-7.
- [29] J. G. Proakis and M. Salehi, *Digital communications*. India: McGraw-Hill India, 2008.
- [30] A. Bessate and F. El Bouanani, "A new performance results of MIMO system with orthogonal STBC over independent and identical weibull fading channels," in *2016 International Conference on Advanced Communication Systems and Information Security (ACOSIS)*, Oct. 2016, pp. 1–7, doi: 10.1109/ACOSIS.2016.7843947.
- [31] M. A. Kumar and J. Ravindra, "4x4 MIMO Alamouti Decoder Implementation Using VERTEX2," *International Journal & Magazine of Engineering, Technology, Management and Research*, vol. 3, no. 12, pp. 67–73, 2016.
- [32] B. Ripan, K. Roy, and T. K. Roy, "BER Analysis of MIMO-OFDM System using Alamouti STBC and MRC Diversity Scheme over Rayleigh Multipath Channel," *Global Journal of Researches in Engineering Electrical and Electronics Engineering*, vol. 13, no. 13, pp. 14–24, 2013.
- [33] C. F. Mecklenbräuker and M. Rupp, "Generalized Alamouti Codes for Trading Quality of Service against Data Rate in MIMO




- UMTS,” *EURASIP Journal on Advances in Signal Processing*, vol. 2004, no. 5, pp. 662–675, Dec. 2004, doi: 10.1155/S1110865704310061.
- [34] N. S. Ali, K. K. Abdalla, and S. A. Kadhim, “BER Performance Improvement of Alamouti MIMO-STBC Decoder Using Mutual Information Method,” *Journal of Physics: Conference Series*, vol. 1530, pp. 1–8, May 2020, doi: 10.1088/1742-6596/1530/1/012016.
- [35] E. Kusumawardhani, R. P. Astuti, N. M. Adriansyah, F. Imansyah, and L. S. A. Putra, “Performance Analysis of Multiple Input Multiple Output (MIMO) Multi-Carrier Code-Division Multiple Access (MC-CDMA) Combined with Quasi-Orthogonal Space Time Block Coding (QO-STBC) in Rayleigh Fading Channel,” *POSITRON*, vol. 12, no. 2, pp. 120–125, Nov. 2022, doi: 10.26418/positron.v12i2.46613.

BIOGRAPHIES OF AUTHORS






Nader Abdullah Kadhim    was born in Babylon, 1962, Iraq. He received the B.Sc. degree in Department Electronics and Communications from the University of Baghdad (1995), Iraq, M.Sc. and Ph.D. degrees in Electronics and Communication Engineering from the University of Technology, Iraq in 2001 and 2007 respectively. Since 2003, he has been with the University of Babylon, Iraq, where he is now head of Department of Electrical Engineering. He can be contacted at email: nader.abdallah@mustaqbal-college.edu.iq.



Ali Jawad Kadhim Jawad Alrubaie    was born in Babylon in 1995. He is graduated from bachelor's degree in Electrical Engineering on 12/7/2017 and obtained a master degree in Electrical Engineering on 12/1/2019 from the University Malaysia Perlis (UniMap). He is research contributions in the field of sustainable energy system, DC system design, and new control systems. He can be contacted at email: eng.ali.jawad@uobabylon.edu.iq.



Osama Qasim Jumah Al-Thahab    was born in Iraq, Babil, AlHilla City, Al-Tayara Quarter 1978. He received the B.Sc. from Babylon University in General Electrical Engineering 2000. The M.Sc. and Ph.D. are in Electronics and Communications field from University of Technology, Iraq 2003 and 2007 respectively. Since 2019, he has been a professor with the Department of Electrical Engineering, Babylon University. He interested in the field's microcontroller, image processing, quad copter, home automation, speech analysing, digital design, and computer software. Also, until know he has 22 articles in these fields. He can be contacted at email: eng.osama.qasim@uobabylon.edu.iq.